NANO LETTERS

2008
Vol. 8, No. 3
810-815

Chemical Synthesis and Magnetotransport of Magnetic Semiconducting $Fe_{1-x}Co_xSi$ Alloy Nanowires

Andrew L. Schmitt, Jeremy M. Higgins, and Song Jin*

Department of Chemistry, University of Wisconsin—Madison, 1101 University Avenue, Madison, Wisconsin 53706

Received October 22, 2007; Revised Manuscript Received January 7, 2008

ABSTRACT

We report single-crystal nanowires of magnetic semiconducting $Fe_{1-x}Co_xSi$ alloys synthesized using a two-component single source precursor approach. Extending our previous syntheses of FeSi and CoSi nanowires from $Fe(SiCl_3)_2(CO)_4$ and $Co(SiCl_3)(CO)_4$ precursors, we found that a homogeneous solution formed upon mixing these two precursors due to melting point suppression. This liquid constitutes the single-source precursor suitable for delivery through chemical vapor deposition, which enables the chemical synthesis of $Fe_{1-x}Co_xSi$ alloy nanowires on silicon substrates covered with a thin (1–2 nm) SiO_2 layer. Using scanning and transmission electron microscopy and energy dispersive X-ray spectroscopy and mapping, we demonstrate two homogenously mixed alloy nanowire samples with very different Co substitution concentrations (x): 6 ± 5%, the ferromagnetic semiconductor regime, and 44 ± 5%, the helical magnetic regime. The magnetotransport properties of these alloy nanowires are pronouncedly different from that of the host structures FeSi and CoSi, as well as from one another, and consistent with the physical properties as expected for their corresponding compositions. These novel magnetic semiconducting silicide nanowires will be important building blocks for silicon-based spintronic nanodevices.

Spintronics seeks to exploit electron spin properties instead of or in addition to charge degrees of freedom in solid-state electronic and photonic devices.[1] Giant magnetoresistance, the early and exemplary development of spintronics, has greatly increased the information storage density in magnetic hard drives and has been recently recognized by the 2007 Nobel Prize in Physics. The full realization of spintronics with the ability to inject, manipulate, and detect electron spins in semiconductor devices[1] will revolutionize computing by offering the advantages of nonvolatility, faster data processing speed, low power consumption, and high integration densities. Despite a long spin coherence lifetime[2] and well-developed materials processing, silicon-based spintronics is much less developed compared with that based on the more popular $Ga_{1-x}Mn_xAs$ dilute magnetic semiconductor (DMS),[3] mainly because of the slow advances in silicon-based magnetic semiconductor materials.[4] This has been changed by the recent discovery of magnetic semiconducting silicide alloys of $Fe_{1-x}Co_xSi$ ($0 < x < 1$),[5,6] which belong to isostructural $B20$ metal monosilicides of highly correlated electron systems (MSi, M = Fe, Co, Mn).[5–9] FeSi and CoSi form a homogeneous solid solution throughout the whole composition range as evidenced by their pseudobinary phase diagram (Figure S1).[10] CoSi is a diamagnetic metal and FeSi is a paramagnetic semiconductor, a so-called Kondo insulator; strangely however, for each Co atom mixed into the FeSi host lattice, one additional Bohr magneton is added to the net magnetization.[5,6,8] The resulting $Fe_{1-x}Co_xSi$ series displays a myriad of magnetic behaviors including that of a ferromagnetic semiconductor (concentrated, not dilute) and a half-metal,[5,11] while displaying an unusual helimagnetic ordering.[12] These silicides are ideal candidates for spin injection into silicon, not only because of their large electron spin polarization and low-to-intermediate carrier density but also because silicides are ubiquitous at interfaces between silicon and metals and widely used as contact and interconnect in the current CMOS microelectronics.[13]

We hope to explore nanowires (NWs) of magnetic semiconducting $Fe_{1-x}Co_xSi$ silicides and silicide−silicon nanowire heterostructures as building blocks to fabricate silicon-based spintronic nanodevices to realize spin injection and detection in silicon. High-quality single crystal NWs provide a promising alternative to conventional top-down fabrication processes in defining nanoscale spintronic devices. There has been much recent work on nanowire materials of *dilute* magnetic semiconductors (DMS).[14,15] However, we are most interested in exploring those *concentrated* magnetic semiconducting nanomaterials, such EuO[16] and EuS NWs,

* Corresponding author: jin@chem.wisc.edu.

10.1021/nl072729c CCC: $40.75
Published on Web 02/01/2008

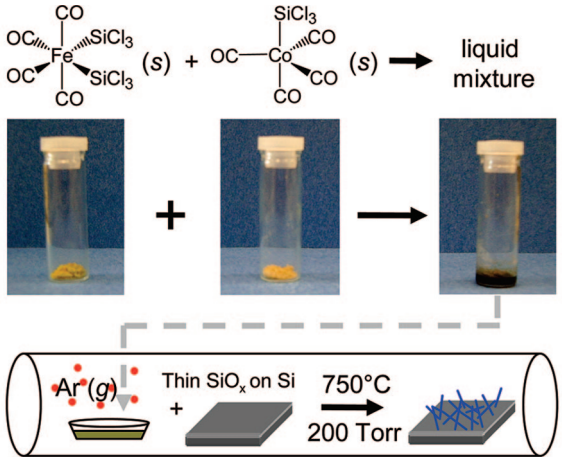

Figure 1. Chemical synthesis of $Fe_{1-x}Co_xSi$ alloy nanowires using CVD of a mixture of two single source precursors. The homogeneous solution of two independent precursors formed upon mixing is vaporized and carried downstream in the CVD reactor by argon gas at a flow rate of 150 sccm, where decomposition and silicide nanowire formation occur on silicon substrates coated with thin (1–2 nm) silicon oxide.

and silicide alloy NWs, not only because of their stronger magnetism and higher spin polarization but also because recent experiments concerning the clustering of dopant and the role of magnetic impurities have cast questions on many initially claimed DMS materials.[15,17] In this Letter, we report the chemical synthesis of magnetic $Fe_{1-x}Co_xSi$ alloy nanowires in order to enable the exploration of silicon-based spintronic nanodevices.

Although nanowire materials have been extensively investigated in the past decade,[18] free-standing nanowires of metal silicides have only recently begun to receive some attention.[19–26] In many of these reported syntheses, either the metal elements (as metal halides or evaporated metal vapors)[24,25] or the silicon precursors[26] were delivered to the substrate in the vapor phase while the solid substrates provided the remaining reactant necessary for silicide nanowire formation. To achieve good chemical control in the nanophase formation of complex intermetallic silicide materials, we have strived to deliver both the metal and silicon elements via the vapor phase by using either chemical vapor deposition of organometallic single source precursors (SSPs)[20–22] or a chemical vapor transport method.[23] The single source precursor approach is particularly suited for the preparation of alloy nanowires as it allows for more reproducible and flexible control over precursor delivery at low temperature with simple experimental setups.[27] Herein, we build on our previous success in synthesizing freestanding FeSi and CoSi NWs by decomposing *trans*-$Fe(SiCl_3)_2(CO)_4$ and $Co(SiCl_3)(CO)_4$ SSPs, respectively, onto silicon substrates covered with a thin (1–2 nm) layer of silicon oxide without the use of metal catalysts.[20–22] We discovered that these two precursors have a favorable intermolecular interaction, resulting in a substantial melting point depression to near room temperature upon mixing. When placed in the same vial, the two solid precursors melt to form a homogeneous solution (Figure 1). After the initial heat of solution had dissipated, the precursors resolidified into the two original and distinct solids, suggesting that a phase change and not a chemical reaction had taken place. In our general synthetic scheme shown in Figure 1, this molecularly mixed solution is used as the new "single-source" precursor (but not single *molecule* precursor) to synthesize $Fe_{1-x}Co_xSi$ NWs by simultaneously delivering Fe, Co, and Si elements in a single CVD gas flow channel to silicon substrates. In such a system, the vapor pressure of the individual components theoretically can be controlled by the ratio of the different molecules in solution together with temperature and external pressure. For an ideal solution the vapor pressure of a given component (p_a) should follow Raoult's law, $p_a = x_a\, p_a^*$, where p_a^* is the vapor pressure of the pure component and x_a is the mole fraction of the component in the solution. Nonlinearity is expected when the components are strongly interacting. It should be noted that resulting NWs will not necessarily have the same metal composition as in the vapor, because the rates of incorporation into the solid could be different. However, we expect that exploratory synthesis will ultimately allow us to control, at least empirically, the degree of substitution (x) by the cobalt atoms in the isostructural FeSi host lattice.

NW syntheses were carried out in a home-built chemical vapor deposition (CVD) reactor comprised of a 1 in. fused silica tube placed in a single-zone tube furnace (Lindberg\Blue M). The sealed tube is equipped with pressure and gas flow controls and a liquid nitrogen trap before the vacuum pump. $Fe(SiCl_3)_2(CO)_4$ and $Co(SiCl_3)(CO)_4$ were synthesized as previously reported,[20,22] mixed in a vial, and then placed in an alumina boat for vaporization upstream of the sealed tube right outside of the furnace. Silicon substrates that have been prepared to have a 1–2 nm silicon oxide coating were placed in the hot zone of the heated tube, 1 in. upstream of the center of the furnace. (See complete synthetic details in the Supporting Information.) Numerous experiments using various ratios of precursor mixtures and different SSP vaporization temperatures (SSP boat position) and CVD reaction temperatures were examined. We will focus on two representative samples in this letter: sample A was prepared with a precursor mixture having a 5:4 mol ratio of Co to Fe at the reaction temperature of 700 °C; sample B was prepared with a precursor mixture having a 5:2 mol ratio of Co to Fe at the reaction temperature of 750 °C.

The resulting freestanding nanowires as grown on substrates were imaged using scanning electron microscopy (SEM) with a LEO Supra field-emission electron microscope or a Carl Zeiss Crossbeam microscope. Representative images of sample A (Figure 2a) and sample B (Figure 2b) show straight NWs but with slightly rough surfaces. No catalyst balls were seen at the tips of nanowires (Figure 2, insets) in agreement with what we have previously found to be true for FeSi,[20] CoSi,[22] and other silicide NWs[23] and suggesting that this growth does not proceed via the common vapor–liquid–solid NW growth mechanism.[28] The $Fe_{1-x}Co_xSi$ nanowires in both samples are long (greater than 10 μm) with diameters between 30 and 60 nm.

The structure and composition of the NWs were determined by high-resolution transmission electron microscopy (HRTEM)

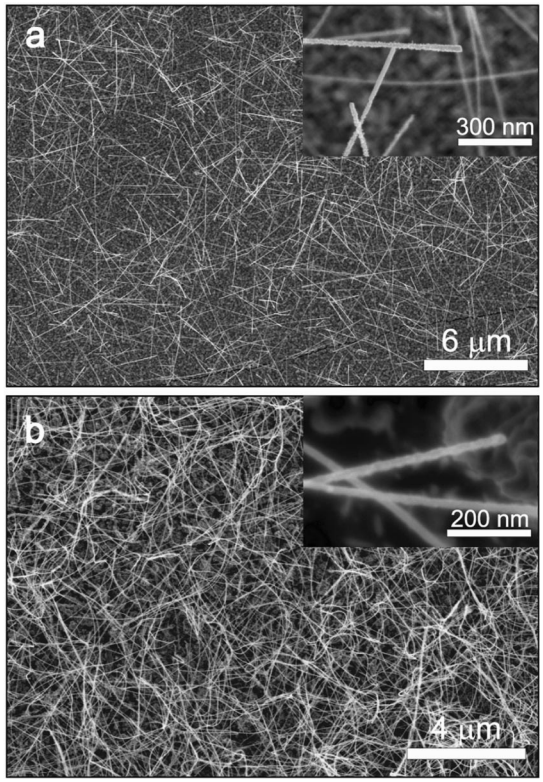

Figure 2. Representative SEM images of $Fe_{1-x}Co_xSi$ nanowires (a) for sample A and (b) for sample B. The magnified insets highlight the tips of the nanowires.

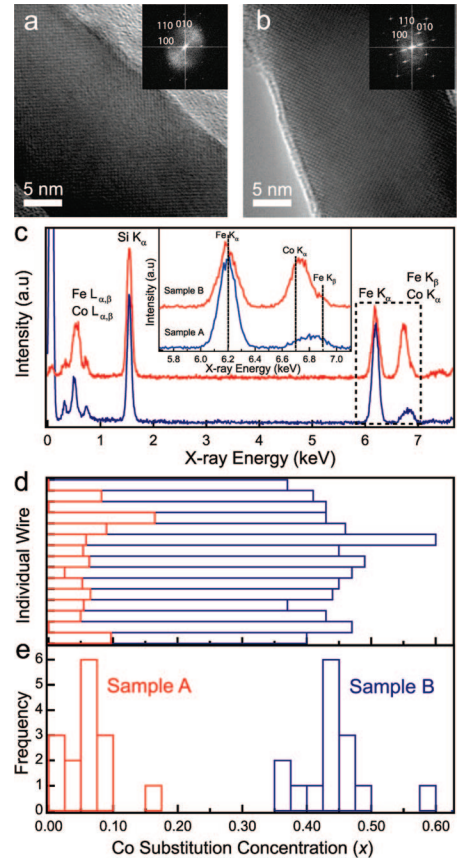

Figure 3. HRTEM and EDX analysis of $Fe_{1-x}Co_xSi$ nanowires. Representative lattice-resolved HRTEM images of $Fe_{1-x}Co_xSi$ nanowires for sample A (a) and for sample B (b). Both insets show indexed FFT along the [100] zone axis. (c) EDX spectra, normalized to the Si K_α signals, from the wires in sample A, lower, blue curve, and sample B, upper, red curve. Inset highlights the metal K edges where the differences in Co substitution are most obvious. (d) The results of EDX analyses (x) and (e) histograms for 15 nanowires each from sample A, red bars, and sample B, blue bars.

and elemental analysis using energy dispersive X-ray spectroscopy (EDX) on single nanowires. HRTEM images were collected using a Philips CM200 UT TEM with an accelerating voltage of 200 kV on NWs that were sonicated and suspended in ethanol and then dispersed onto lacey carbon film TEM grids. The limiting members of the $Fe_{1-x}Co_xSi$ alloys, FeSi and CoSi, are isostructural with a simple cubic lattice type (space group $P2_13$, Person symbol $cP8$, structure type FeSi, $Z = 4$) with a lattice constant of 4.488 Å for FeSi (JCPDS PDF00-038-1397) and 4.43 Å for CoSi (JCPDS PDF00-008-362), respectively.[29] In bulk, FeSi and CoSi form a disordered homogeneous solution of FeSi and CoSi in the whole range ($0 \leq x \leq 1$) (see Supporting Information). HRTEM images show cubic lattice fringes of the FeSi host structure for a representative $Fe_{1-x}Co_xSi$ nanowire along the [100] zone axis for each sample (Figure 3a for sample A, Figure 3b for sample B). The corresponding fast Fourier transformations (FFT) (Figure 3a,b, Insets) are indexed to a cubic lattice. All NWs observed under TEM were single crystalline and could be indexed to the FeSi structure. The preferential growth axis of all NWs observed using TEM were parallel to the ⟨110⟩ crystal directions. This is the same growth habit observed for the FeSi and CoSi NWs made using our SSP approach but different from the FeSi and CoSi NWs prepared using metal halide precursors with silicon substrates.[24] It is evident that the nanowire surfaces are covered with a thin (2–3 nm) amorphous layer that is reasonably attributed to silicon oxide based on the known surface oxidation of silicides.[30] The observed [100] lattice spacings of 4.49 Å for sample A and 4.51 Å for sample B are close to the 4.488 Å value reported for FeSi. If we indeed have made NWs of the alloys, Vergard's law would yield the expectation that the lattice constants would fall between 4.43 and 4.488 Å. However, the accuracy of the lattice measurements based on FFT calculations cannot resolve such a small lattice offset (4%). Nonetheless, the HRTEM experiments clearly show that the host structure of the alloys are intact with only one single-crystalline phase observed in each nanowire.

EDX was performed on the same nanowires to verify the elemental composition for both samples (Figure 3c). The bottom curve (blue) corresponds to sample A, whereas the upper curve (red) corresponds to sample B. It is difficult to resolve the L edges since the energy difference between the Fe L_2 and the Co L_2 edge is merely 70 eV; however, their K edges are separated by 500 eV (Figure 3c, Inset). For sample A the Fe signal is strong and only a minimal peak is observed for the main Co K edge, seen as the shoulder for the second peak. For sample B, both the Fe K edge and the Co K edge are obviously present with similar magnitude. This subtle but definitive difference is the basis for the quantification of the Fe:Co ratios.

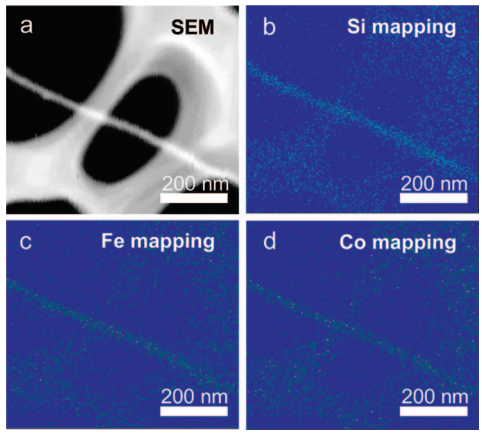

Figure 4. EDX mapping of an alloy nanowire: (a) the SEM image of the nanowire dispersed on a lacey carbon TEM grid and the elemental mapping of (b) the Si K edge, (c) Fe K edge, and (d) Co K edge.

To ensure the statistical significance of the elemental analysis and to determine the possible variation from one nanowire to the next in a given synthetic run, further EDX analyses on many more nanowires randomly selected from each sample pool were carried out to determine the Co substitution level, x, in these $Fe_{1-x}Co_xSi$ alloy nanowires. These EDX spectra were collected using a Carl Zeiss Crossbeam SEM on single nanowires. Figure 3d shows the EDX results on the individual nanowires from sample A (red) and sample B (blue). Figure 3e represents the same data in the form of a histogram of the x parameter of the 15 spectra taken on sample A (red, left) and sample B (blue, right). The distributions of each sample fall roughly within a 10% window and are centered about 6% for sample A and 44% for sample B; i.e., the statistical analysis shows the NWs from sample A have the composition of $Fe_{0.94}Co_{0.06}Si$ and the NWs from sample B have the composition of $Fe_{0.56}Co_{0.44}Si$. Note that the quantitative error for typical standardless EDX analysis is approximately 5%, but the statistical standard deviation of the mean for sample A (B) is 4.2% (5.5%). The compositions of Fe and Co determined using the HRTEM−EDX spectra are in line with these more extensive analyses. The compositional ranges described in these samples should correspond to a ferromagnetic semiconductor ($x = 0.06$, sample A) and a helical magnet ($x = 0.44$, sample B) based on measurements in bulk samples with similar concentrations.[5]

We performed an elemental mapping of the Co, Fe, and Si in the $Fe_{1-x}Co_xSi$ alloy NWs to probe their alloying homogeneity. For NWs analyzed in this way, the SEM image (Figure 4a) is reconstructed in the spatial mapping of all three elemental K lines as the electron beam is rastered across the nanowire (Figure 4b−d). Clearly all three elements (Fe, Co, and Si) are present throughout the NWs. We need to point out that the excited volume of the electron beam at the operating voltage (14 kV) is fairly large and the resolution of this kind of elemental mapping cannot ensure *atomic-scale* homogeneity. While it is still possible that atomic segregation can occur, this is unlikely due to the single crystalline nature of the nanowires and the single phase, solid solution nature expected from the pseudobinary phase diagram (see Figure S1) and due to the observed physical properties consistent with the corresponding bulk alloy phases (vide infra). A very effective analytical technique to determine three-dimensional chemical composition mapping with single-atom sensitivity and subnanometer spatial resolution is atom probe tomography (APT),[31] as recently demonstrated with an impressive APT analysis of metal impurities in nanowires.[32] We are developing analytical methods to *conclusively* demonstrate the homogeneous alloy distribution in $Fe_{1-x}Co_xSi$ NWs using APT.

Room-temperature electrical transport of the $Fe_{1-x}Co_xSi$ NWs was investigated by measuring two- and four-terminal devices. For device fabrication, alloy NWs were first suspended in ethanol via sonication and deposited onto degenerately doped Si(100) substrates coated with 600 nm of thermally grown silicon oxide. Electrodes were then defined using e-beam lithography, and nonmagnetic metal contacts to NWs were made using e-beam evaporated 40 nm Au atop 40 nm Ti after a 5 s 5% HF etch. Measurements were carried out using a probe station and a home-built transport measurement setup. Four probe device studies indicate that substantial contact resistance, more than 100 Ω, was rarely seen and is only present when the two-terminal I–V measurement was nonlinear (see Supporting Information and Figure S3). On the basis of this assessment we used the resistance from 8 (13) two terminal devices made out of $Fe_{1-x}Co_xSi$ nanowires from sample A (B) and the corresponding SEM micrographs of the devices to determine the average resistivity for each sample (see Tables S1 and S2). The resistivity of sample A (B) was 2.49 mΩ cm (2.56 mΩ cm) with a standard deviation of 1.73 mΩ cm (1.21 mΩ cm) as described in more detail in the Supporting Information. These values are approximately 1 order of magnitude larger than the reported values for the pure FeSi and CoSi NWs and for bulk alloy samples.[20,22] The reason for this difference in resistivity which is clearly intrinsic to the single crystalline nanowires (not the result of contact resistance) is unknown to us at present.

In order to highlight the physical property dependence on Co concentration, we examined the differences in magnetoelectrical transport properties of sample A and sample B. Low-temperature measurements were performed on two-terminal Al wire bonded devices using a Quantum Design Physical Property Measurement System (PPMS) and a Keithley 2400 sourcemeter. For devices with linear I–V curves, and hence little to no contact resistance, resistivity was measured as a function of temperature and of transverse applied magnetic field. Figure 5 shows the results of the measurements made on typical devices for $Fe_{1-x}Co_xSi$ alloy NWs of both sample A (Figure 5a−c) and sample B (Figure 5d−f). The resistivities of the NW devices were calculated with the diameter and length of NWs measured using SEM after the device measurements were taken. The room temperature resistivity values for the low temperature devices of both sample A ($x = 0.06$) and sample B ($x = 0.44$) (which are in the mΩ cm range) fall within a standard deviation of their calculated averages presented above. The line shape of the resistivity versus temperature plot for both samples with and without applied magnetic fields is expected and

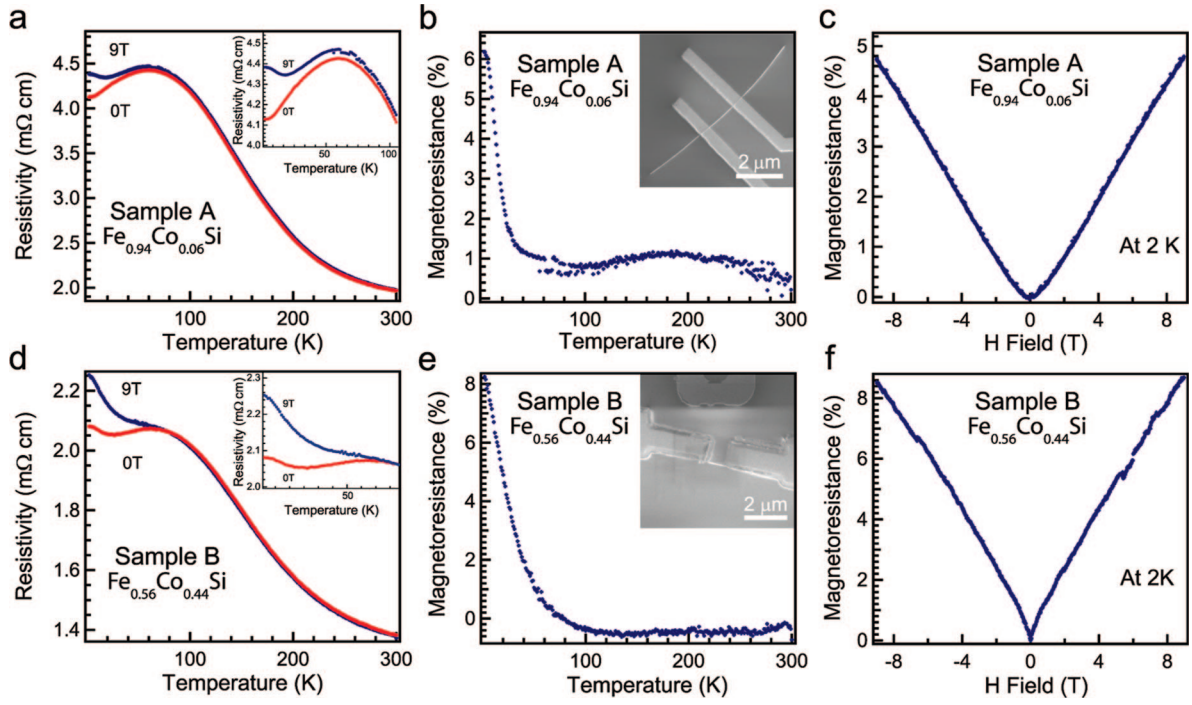

Figure 5. Magnetotransport measurements of representative $Fe_{1-x}Co_xSi$ alloy nanowire devices for sample A ($x = 0.06$) and sample B ($x = 0.44$). (a) and (d) Resistivity as a function of temperature with (blue curve) and without (red curve) applied magnetic field of 9 T for samples A and B, respectively. Insets show the region of interest where the traces split. (b) and (e) MR calculated from the traces in a and d for samples A and B, respectively. Insets show the SEM images of the single nanowire devices measured. (c) and (f) Magnetic field dependence of the magnetoresistance for samples A and B at 2 K.

qualitatively similar to previous bulk measurements. The transition from semiconducting to metallic behavior in the R versus T curves (Figure 5a,d) is indicative of narrow bandgap semiconductors and has been observed in the analogous bulk samples.[8] The observed magnetoresistance (MR) was positive in both cases (Figure 5b,e), which is expected for the $Fe_{1-x}Co_xSi$ alloys,[8] but different from the host material FeSi[9] (see Supporting Information). At 2 K, the MR versus field strength for sample A (B) has maximum of 4.9% (8.7%) at the highest magnetic field of 9 T (Figure 5c,f). This large MR is in line with previous reports for the bulk materials. The onset of the large MR in sample A occurs at a much lower temperature (15 K) than for sample B (50 K), which is expected due to the higher T_c reported for bulk samples with higher Co concentrations (but only up to 50%).[8] The clear shape difference in the MR versus field curves (Figure 5c,f) between sample A and sample B also indicates that there is a fundamental difference between the physical behaviors of these samples that stems from the different levels of Co incorporation. The different physical properties observed for these two presented samples verify that we have successfully created alloy NWs that are not only physically distinctive from the FeSi and CoSi host materials but also different from one another. The fact that these properties follow the expectations from the bulk materials of comparable compositions indirectly confirms that homogenously alloyed (doped) silicide nanowires of $Fe_{1-x}Co_xSi$ have been successfully synthesized over a large composition range (at least 0.06−0.44). These nanoscale building blocks are ferromagnetic semiconducting, expected to be in a helical magnetic ground state, and have great potential to provide spin polarized current for silicon based spintronic nanodevices.

With regard to the difference between many synthetic conditions, including those for sample A and sample B, it does generally appear that the higher the Co percentage in the SSP mixtures, the more likely Co will show up with higher concentrations in the resulting NWs. We could not determine whether or not the temperature change, such as from 700 °C (sample A) to 750 °C (sample B), had a large effect on the amount of Co incorporated, because we have not seen strong dependence of x to reaction temperature in similar experiments. It also should be noted that some regions of the sample B substrate were found to contain shorter, fatter nanowires with diameters larger than 80 nm (Figure S2b). An EDX study (Figure S2a) suggested these thicker wires have the composition of Co_2Si (a full characterization of this impurity is ongoing). This impurity seen in sample B, made at higher reaction temperature, is attributed to the extra $Co(SiCl_3)(CO)_4$ precursor in the system near the end of the reaction time after the FeSi source is depleted. No such impurity phase has thus far been found in sample A made at lower temperature. The sensitive dependence to different reaction conditions and/or the complexity of vapor–liquid phase equilibrium in this nonideal liquid-phase precursor mixture have not yet allowed the strict and reproducible control of the Fe to Co ratio in NW products at a satisfying level, which is the area we are working to improve upon. Nonetheless, the fact that we have prepared alloy NWs with distinctively different compositions points to the fundamental possibility that with more optimization of the process, refined instrumental control, and better understanding of growth

conditions, ultimately one can controllably prepare NWs with the desired doping levels at will. In the meantime, we show that the nanowires from a given sample can already be employed for spintronic device fabrication since statistical analyses have shown that within a synthetic run the nanowire composition is relatively uniform (vide supra).

In summary, we have achieved the synthesis of magnetic semiconducting $Fe_{1-x}Co_xSi$ alloy nanowires through an entirely chemical approach using a two-component single source precursor. The host lattice was structurally characterized using HRTEM, and the substitution parameter (x) has been statistically verified to be up to 0.44 using EDX on single nanowires. The magnetotransport investigations of single nanowire devices suggested that two distinct magnetic property regimes, different from the host structures, have been synthetically achieved. Because the magnetic properties of the alloy nanowires are intimately related to metal atomic environments, we are further studying the spatial distribution of Co atoms in the FeSi host lattice at atomic scale using atom probe tomography, and we are investigating the elemental specific contribution to these nanomaterials' magnetic moments using X-ray magnetic circular dichroism (XMCD). Exploration of these novel nanoscale building blocks for silicon-based spintronic nanodevices is also underway.

Acknowledgment. This research was supported by Research Corporation through a Cottrell Scholar Award to S.J., an IEDR Grant, a Draper TIF Grant, and the startup fund provided by UW-Madison. S.J. is a 3M Nontenured Faculty Awardee and a DuPont Young Professor. We thank Professor Mark Eriksson for access to the PPMS.

Supporting Information Available: Details of the nanowire synthesis for both samples, a reprinted pseudobinary phase diagram of FeSi with CoSi, EDX and SEM of the Co_2Si impurity phase in sample B, two- and four-terminal measurements of $Fe_{1-x}Co_xSi$ alloy NWs, average resistivities of both samples at room temperature, and low T electrical measurements for both CoSi and FeSi. This material is available free of charge via the Internet at http://pubs.acs.org.

References

(1) (a) Zutic, I.; Fabian, J.; Das Sarma, S. *Rev. Mod. Phys.* **2004**, *76*, 323–410. (b) Wolf, S. A.; Awschalom, D. D.; Buhrman, R. A.; Daughton, J. M.; Von Molnar, S.; Roukes, M. L.; Chtchelkanova, A. Y.; Treger, D. M. *Science* **2001**, *294*, 1488–1495. (c) Ando, K. *Science* **2006**, *312*, 1883–1885.

(2) (a) Zutic, I.; Fabian, J.; Erwin, S. C. *Phys. Rev. Lett.* **2006**, *97*, 026602/1–026602/4. (b) Appelbaum, I.; Huang, B.; Monsma, D. J. *Nature* **2007**, *447*, 295–298.

(3) Ohno, H.; Shen, A.; Matsukura, F.; Oiwa, A.; Endo, A.; Katsumoto, S.; Lye, Y. *Appl. Phys. Lett.* **1996**, *69*, 363–365.

(4) Pearton, S. *Nat. Mater.* **2004**, *3*, 203–204.

(5) Manyala, N.; Sidis, Y.; Ditusa, J. F.; Aeppli, G.; Young, D. P.; Fisk, Z. *Nat. Mater.* **2004**, *3*, 255–262.

(6) Manyala, N.; Sidis, Y.; DiTusa, J. F.; Aeppli, G.; Young, D. P.; Fisk, Z. *Nature* **2000**, *404*, 581.

(7) (a) Aeppli, G.; DiTusa, J. F. *Mater. Sci. Eng., B* **1999**, *63*, 119–124. (b) Mena, F. P.; DiTusa, J. F.; van der Marel, D.; Aeppli, G.; Young, D. P.; Damascelli, A.; Mydosh, J. A. *Phys. Rev. B* **2006**, *73*, 085205/1–085205/7. (c) Pfleiderer, C.; Reznik, D.; Pintschovius, L.; von Lohneysen, H.; Garst, M.; Rosch, A. *Nature* **2004**, *427*, 227–231.

(8) Onose, Y.; Takeshita, N.; Terakura, C.; Takagi, H.; Tokura, Y. *Phys. Rev. B* **2005**, *72*, 224431/1–224431/12.

(9) Paschen, S.; Felder, E.; Chernikov, M. A.; Degiorgi, L.; Schwer, H.; Ott, H. R.; Young, D. P.; Sarrao, J. L.; Fisk, Z. *Phys. Rev. B* **1997**, *56*, 12916–12930.

(10) Villars, P. ; Prince, A. ; Okamoto, H. , *Handbook of Ternary Phase Diagrams*; American Society for Metals: Metals Park, OH,1995.

(11) Guevara, J.; Vildosola, V.; Milano, J.; Llois, A. M. *Phys. Rev. B* **2004**, *69*, 184422/1–184422/6.

(12) Uchida, M.; Onose, Y.; Matsui, Y.; Tokura, Y. *Science* **2006**, *311*, 359–361.

(13) (a) Zhang, S. L.; Ostling, M. *Crit. Rev. Solid State Mater. Sci.* **2003**, *28*, 1–129. (b) Zhang, S. L.; Smith, U. *J. Vac. Sci. Technol., A* **2004**, *22*, 1361–1370.

(14) (a) Radovanovic, P. V.; Barrelet, C. J.; Gradecak, S.; Qian, F.; Lieber, C. M. *Nano Lett.* **2005**, *5*, 1407–1411. (b) Choi, H.-J.; Seong, H.-K.; Chang, J.; Lee, K.-I.; Park, Y.-J.; Kim, J.-J.; Lee, S.-K.; He, R.; Kuykendall, T.; Yang, P. *Adv. Mater.* **2005**, *17*, 1351–1356.

(15) Kulkarni, J. S.; Kazakova, O.; Holmes, J. D. *App. Phys. A* **2006**, *85*, 277–286.

(16) Bierman, M. J.; Van Heuvelen, K. M.; Schmeisser, D.; Brunold, T. C.; Jin, S. *Adv. Mater.* **2007**, *19*, 2677–2681.

(17) (a) Kim, J. Y.; Park, J. H.; Park, B. G.; Noh, H. J.; Oh, S. J.; Yang, J. S.; Kim, D. H.; Bu, S. D.; Noh, T. W.; Lin, H. J.; Hsieh, H. H.; Chen, C. T. *Phys. Rev. Lett.* **2003**, *90*, 017401. (b) Keavney, D. J.; Buchholz, D. B.; Ma, Q.; Chang, R. P. H. *App. Phys. Lett.* **2007**, *91*, 012501/1–012501/3. (c) Kuroda, S.; Nishizawa, N.; Takita, K.; Mitome, M.; Bando, Y.; Osuch, K.; Dietl, T. *Nat. Mater.* **2007**, *6*, 440–446.

(18) (a) Xia, Y.; Yang, P.; Sun, Y.; Wu, Y.; Mayers, B.; Gates, B.; Yin, Y.; Kim, F.; Yan, H. *Adv. Mater.* **2003**, *15*, 353–389. (b) Samuelson, L.; Thelander, C.; Bjoerk, M. T.; Borgstroem, M.; Deppert, K.; Dick, K. A.; Hansen, A. E.; Martensson, T.; Panev, N.; Persson, A. I.; Seifert, W.; Skoeld, N.; Larsson, M. W.; Wallenberg, L. R. *Physica E* **2004**, *25*, 313–318. (c) Wang, F.; Dong, A.; Sun, J.; Tang, R.; Yu, H.; Buhro, W. E. *Inorg. Chem.* **2006**, *45*, 7511–7521. (d) Lieber, C. M.; Wang, Z. L. *MRS Bull.* **2007**, *32*, 99–108.

(19) Wu, Y.; Xiang, J.; Yang, C.; Lu, W.; Lieber, C. M. *Nature* **2004**, *430*, 61–65.

(20) Schmitt, A. L.; Bierman, M. J.; Schmeisser, D.; Himpsel, F. J.; Jin, S. *Nano Lett.* **2006**, *6*, 1617–1621.

(21) Schmitt, A. L.; Jin, S. *Chem. Mater.* **2007**, *19*, 126–128.

(22) Schmitt, A. L.; Zhu, L.; Schmeier, D.; Himpsel, F. J.; Jin, S. *J. Phys. Chem. B* **2006**, *110*, 18142–18146.

(23) (a) Song, Y.; Jin, S. *Appl. Phys. Lett.* **2007**, *90*, 173122/1–173122/3. (b) Song, Y.; Schmitt, A. L.; Jin, S. *Nano Lett.* **2007**, *7*, 965–969. (c) Szczech, J. R.; Schmitt, A. L.; Bierman, M. J.; Jin, S. *Chem. Mater.* **2007**, *19*, 3238–3243.

(24) (a) Ouyang, L.; Thrall, E. S.; Deshmukh, M. M.; Park, H. *Adv. Mater.* **2006**, *18*, 1437–1440. (b) Varadwaj, K. S. K.; Seo, K.; In, J.; Mohanty, P.; Park, J.; Kim, B. *J. Am. Chem. Soc.* **2007**, *129*, 8594–8599.

(25) (a) Seo, K.; Varadwaj, K. S. K.; Cha, D.; In, J.; Kim, J.; Park, J.; Kim, B. *J. Phys. Chem. C* **2007**, *111*, 9072–9076. (b) Seo, K.; Varadwaj, K. S. K.; Mohanty, P.; Lee, S.; Jo, Y.; Jung, M.-H.; Kim, J.; Kim, B. *Nano Lett.* **2007**, *7*, 1240–1245. (c) Chueh, Y.-L.; Ko, M.-T.; Chou, L.-J.; Chen, L.-J.; Wu, C.-S.; Chen, C.-D. *Nano Lett.* **2006**, *6*, 1637–1644.

(26) (a) Kim, J.; Anderson, W. A. *Thin Solid Films* **2005**, *483*, 60–65. (b) Dong, L. F.; Bush, J.; Chirayos, V.; Solanki, R.; Jiao, J. *Nano Lett.* **2005**, *5*, 2112. (c) Yan, X. Q.; Yuan, H. J.; Wang, J. X.; Liu, D. F.; Zhou, Z. P.; Gao, Y.; Song, L.; Liu, L. F.; Zhou, W. Y.; Wang, G.; Xie, S. S. *Appl. Phys. A* **2004**, *79*, 1853–1856. (d) Kim, C.-J. K. , Kibum; Woo, Yun Sung; Ryu, Kyung-Guk; Moon, Heesung; Kim, Jae-Myung; Zang, Dong-Sik; Jo, Moon-Ho, *Adv. Mater.* Early view..

(27) (a) Barrelet, C. J.; Wu, Y.; Bell, D. C.; Lieber, C. M. *J. Am. Chem. Soc.* **2003**, *125*, 11498–11499. (b) Gleizes, A. N. *Chem. Vap. Deposition* **2000**, *6*, 155–173.

(28) (a) Wagner, R. S.; Ellis, W. C. *Appl. Phys. Lett.* **1964**, *4*, 89–90. (b) Morales, A. M.; Lieber, C. M. *Science* **1998**, *279*, 208–211.

(29) Villars, P.; Calvert, L. D., *Pearson's Handbook of Crystallographic Data for Intermetallic Phases*; 2nd ed.; ASTM International: Newbury, OH, 1991.

(30) Stolt, L.; Thomas, O.; Dheurle, F. M. *J. Appl. Phys.* **1990**, *68*, 5133–5139.

(31) Kelly, T. F.; Larson, D. J.; Thompson, K.; Alvis, R. L.; Bunton, J. H.; Olson, J. D.; Gorman, B. P. *Annu. Rev. Mater. Res.* **2007**, *37*, 681–727.

(32) Perea, D. E.; Allen, J. E.; May, S. J.; Wessels, B. W.; Seidman, D. N.; Lauhon, L. J. *Nano Lett.* **2006**, *6*, 181–185.

NL072729C